SUPPLEMENTARY INFORMATION

Self-triggered conformations of disulfide ensembles in coordination polymers with multiple metal clusters

Tien-Wen Tseng,*[a] Tzuoo-Tsair Luo,[b] Ying-Ru Shih,[ab] Jing-Wen Shen,[ab] Li-Wei Lee,[b] Ming-Hsi Chiang,*[b] and Kuang-Lieh Lu*[b]

[a]Department of Chemical Engineering, National Taipei University of Technology, Taipei 106, Taiwan
[b]Institute of Chemistry, Academia Sinica, Taipei 115, Taiwan

Contents

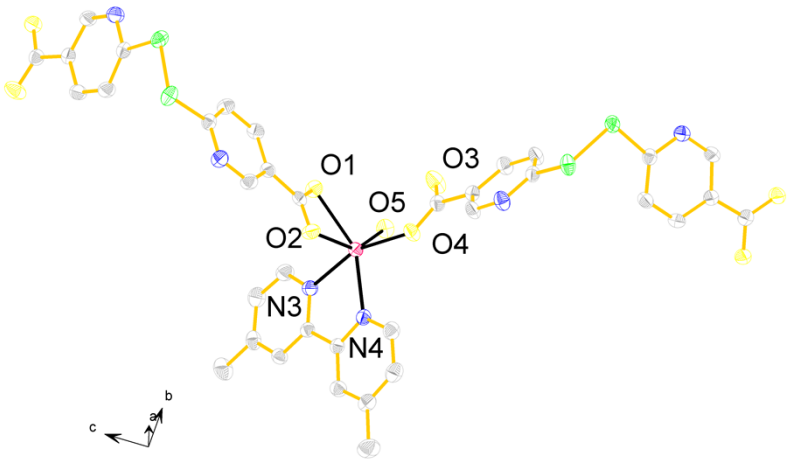

Fig. S1 The ORTEP drawing of **1** with 50% thermal ellipsoid probability. Hydrogen atoms were omitted for clarity.

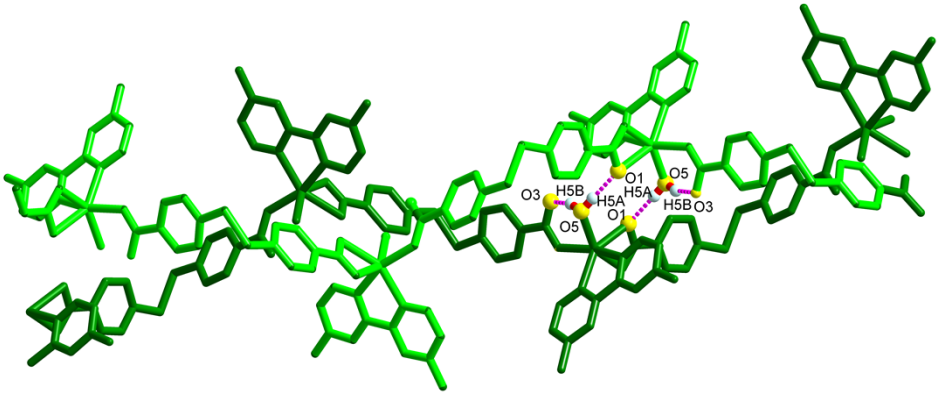

Fig. S2 Two 1D zigzag chains of **1** are paired together via the hydrogen bonding interactions.

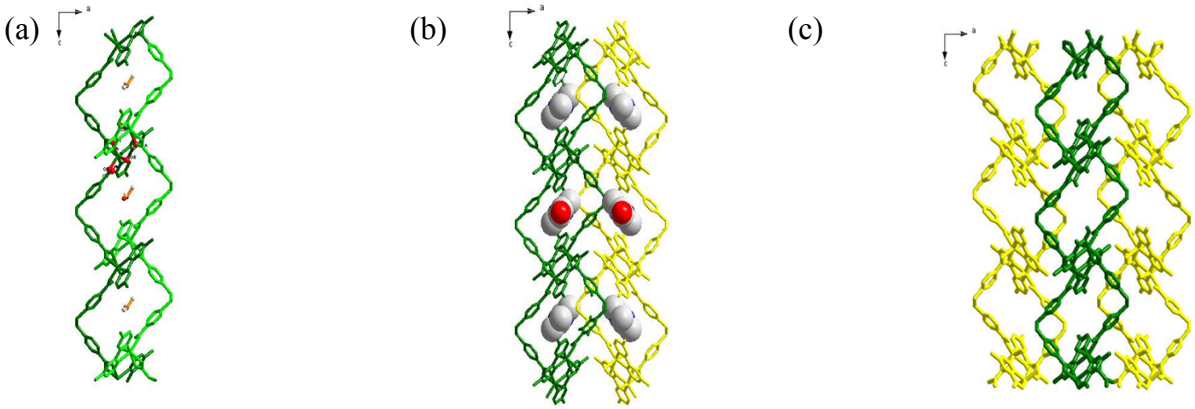

Fig. S3 Structures of **1**: (a) two chains are paired to form a 1D double-stranded ladder viewed along the *a* axis; (b) each cavity is filled with a DMF molecule in space-filling mode viewed along the *b* axis; (c) a 2D framework is stacked with the ladders in an ABAB fashion.

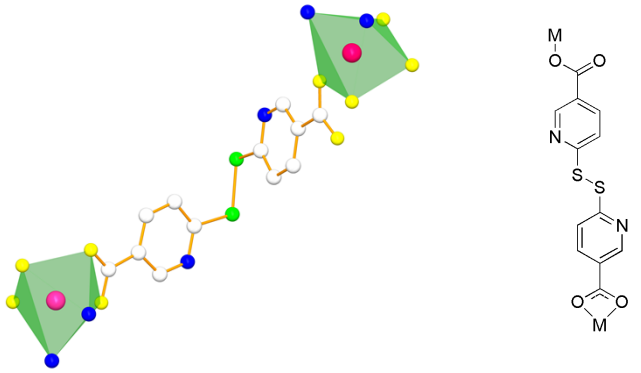

Fig. S4 The coordination mode of the $dtdn^{2-}$ ligand of **1** displays P-form and Type b.

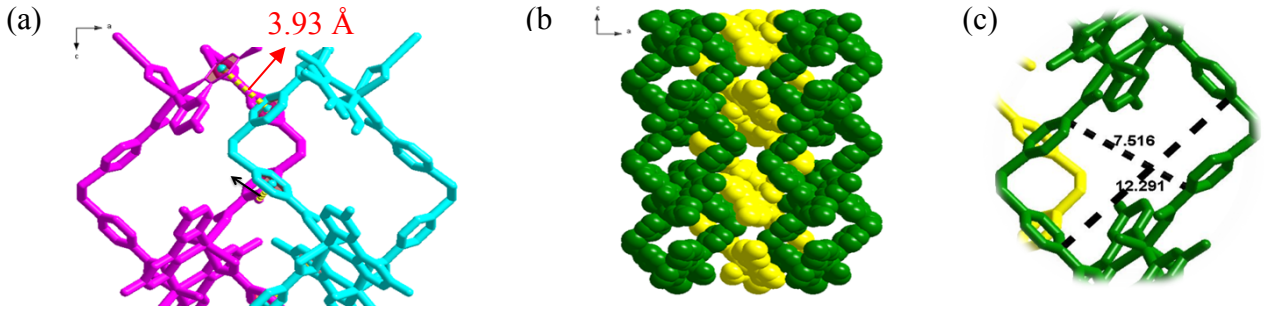

Fig. S5 The structures of compound **1**: (a) showing the π–π stacking interactions with 3.84 Å and 3.93 Å, (b) showing a 2D sheet with the cavities in a space-filling mode, (c) the window size of cavity with 7.52 × 12.29 $Å^2$ and its guest DMF molecule was omitted for clarity.

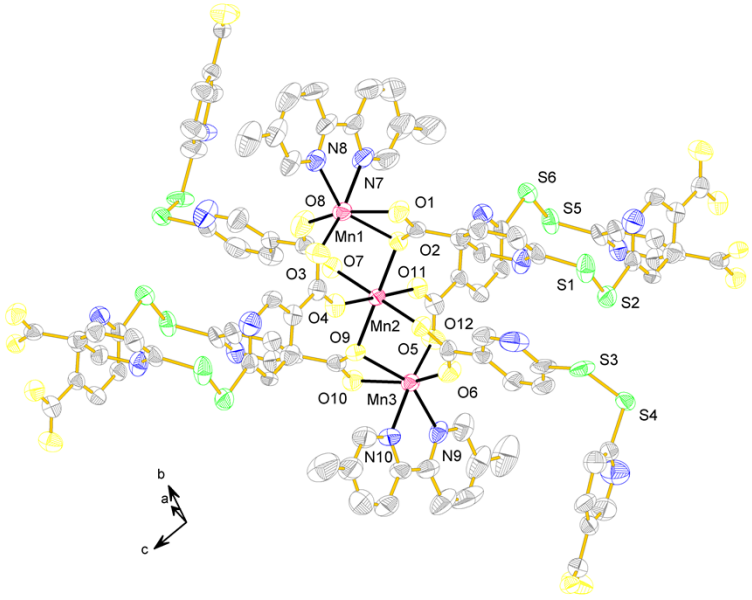

Fig. S6 The ORTEP drawing of **2** with 30% thermal ellipsoid probability. Hydrogen atoms were omitted for clarity.

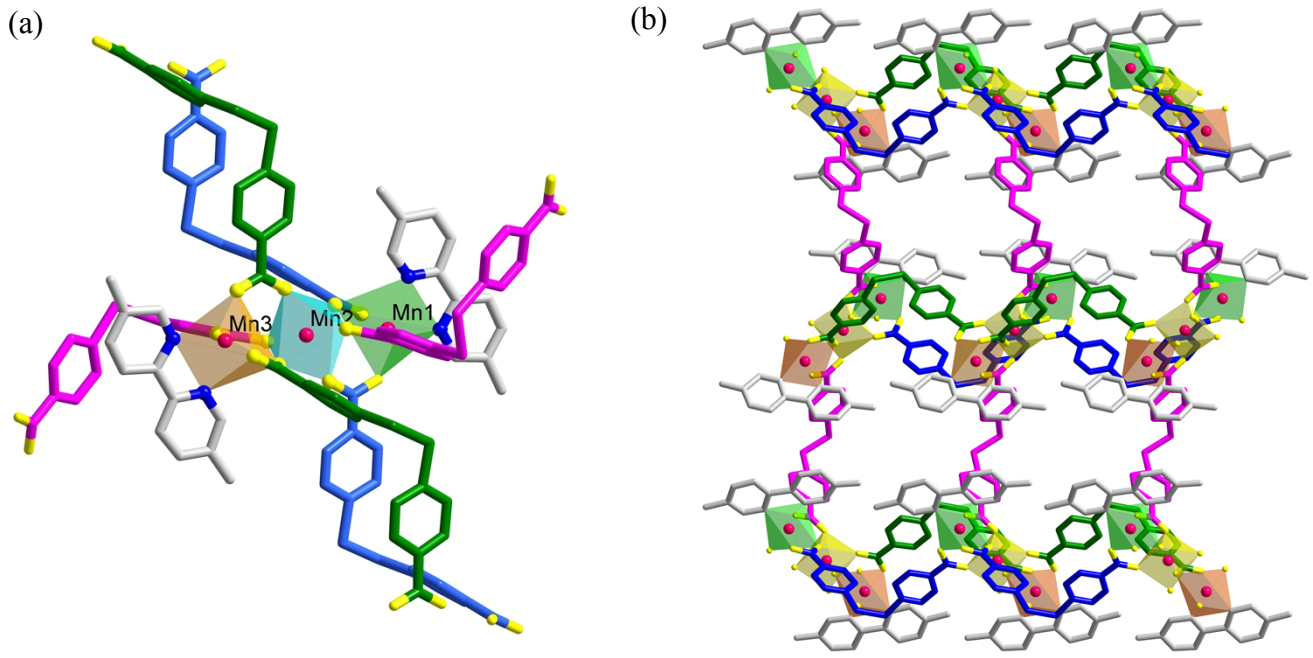

Fig. S7 (a) View of six $dtdn^{2-}$ ligands on a trinuclear cluster of **2** with the separation distances of Mn1···Mn2 and Mn2···Mn3 are 3.55 and 3.57 Å, respectively. (b) Schematic view of a 2D reticular framework along the *c* axis.

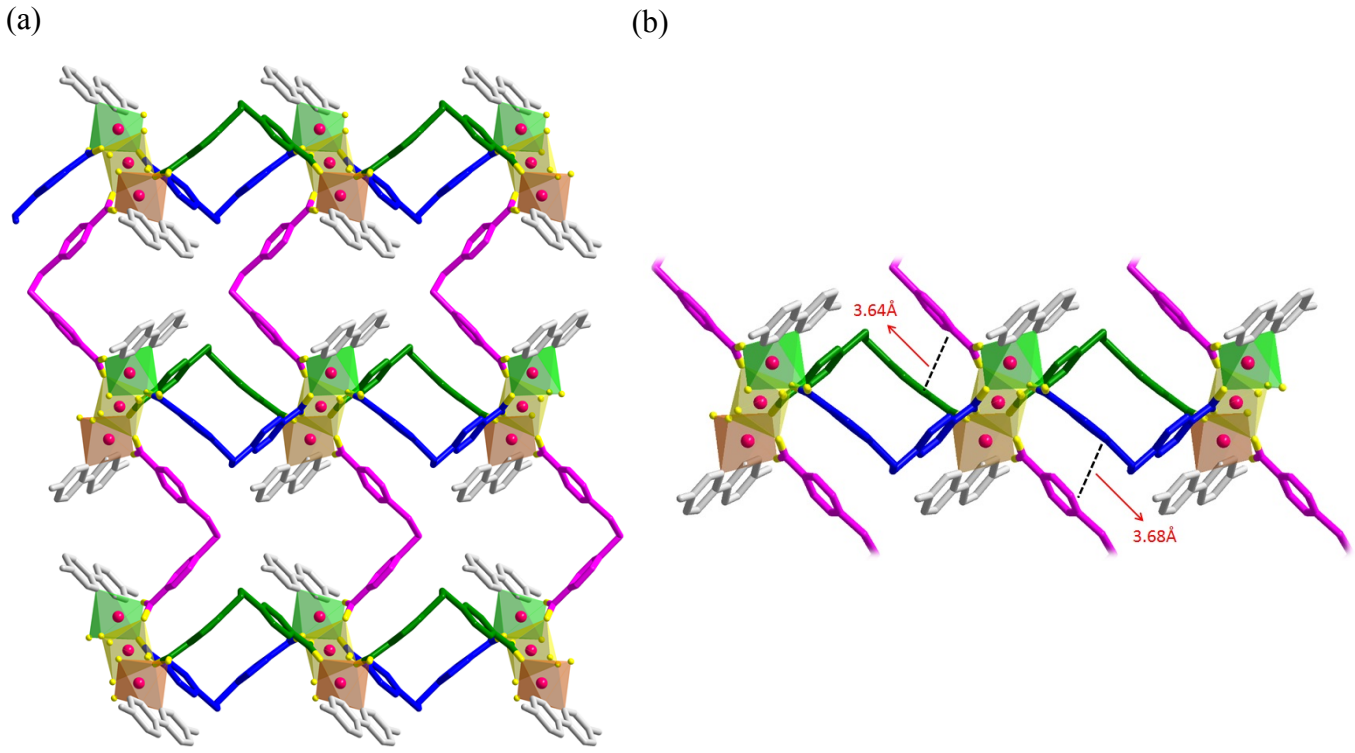

Fig. S8 The structure of **2**: (a) schematic view of a planar structure, (b) a view of π–π stacking interactions.

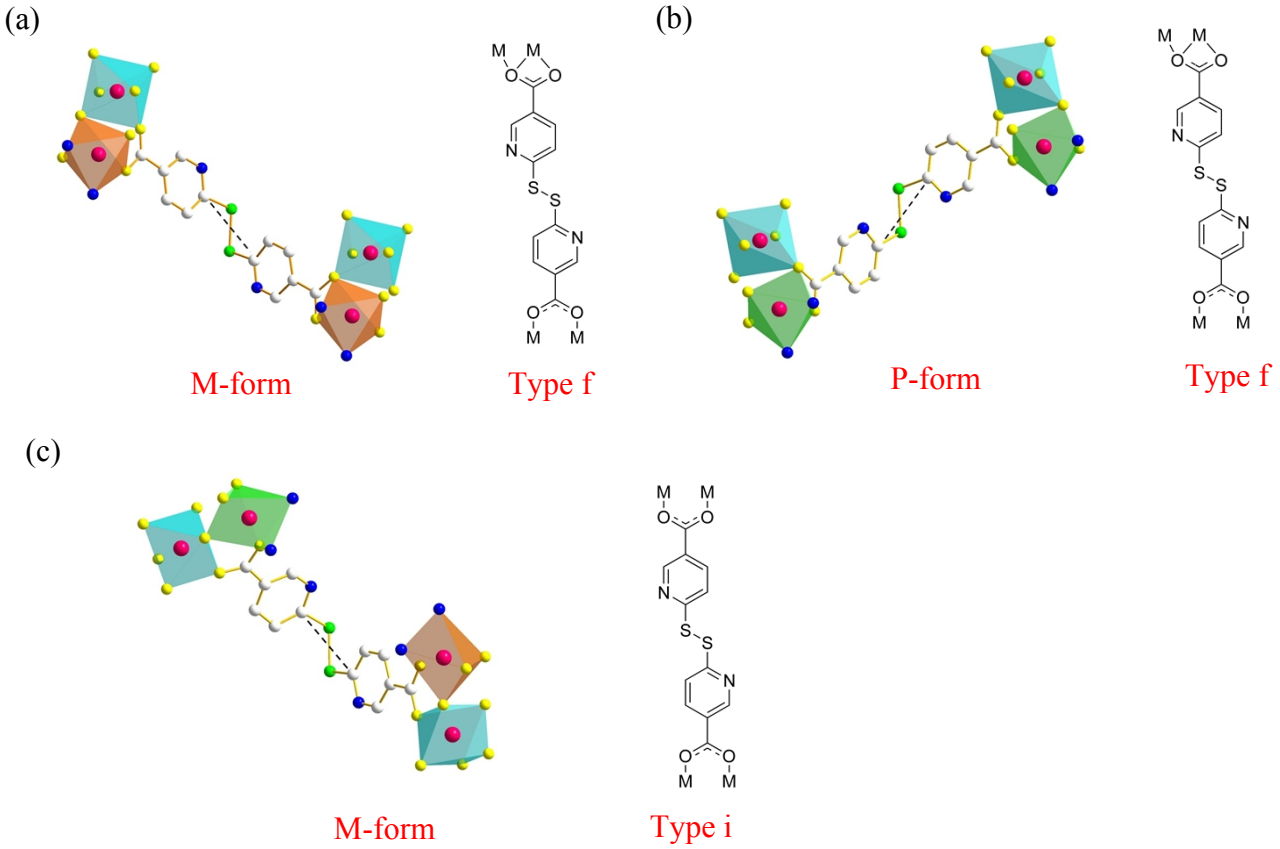

Fig. S9 The structures of **2** show the axial chirality forms, coordination modes, and torsion angles (−C−S−S−C−) of the $dtdn^{2-}$ ligands: (a) M-form, Type (j), 104.2° and 106.1°; (b) P-form, Type (f), 105.4° and 106.3°; (c) M-form, Type (i), 106.6° and 103.1°.

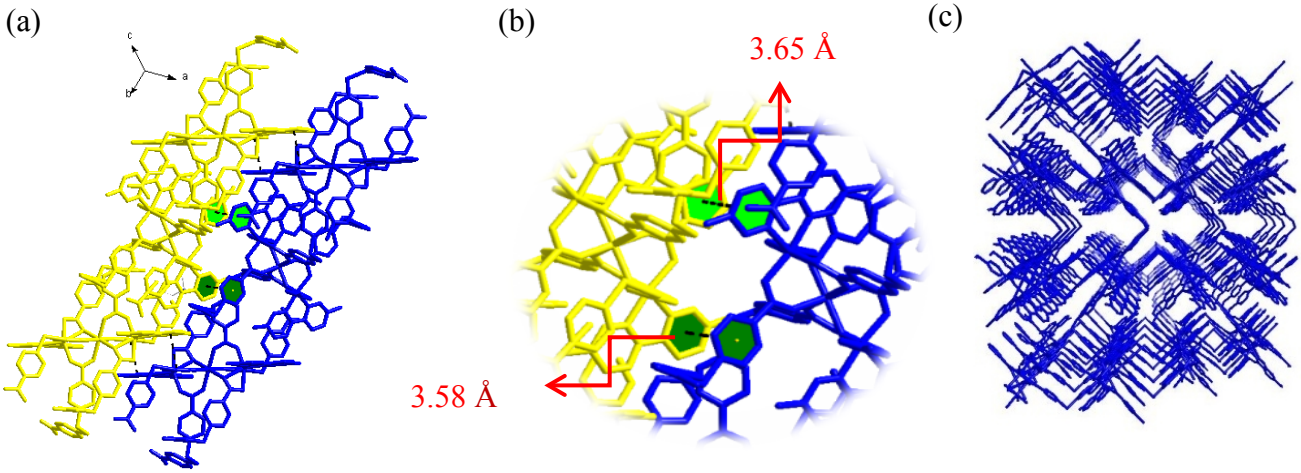

Fig. S10 The structures of **2**: (a) showing the 2D layers are regularly packed into a 3D framework; (b) the π–π stacking interactions are present between two adjacent pyridyl rings of the $dtdn^{2-}$ ligands; (c) a 3D packing diagram.

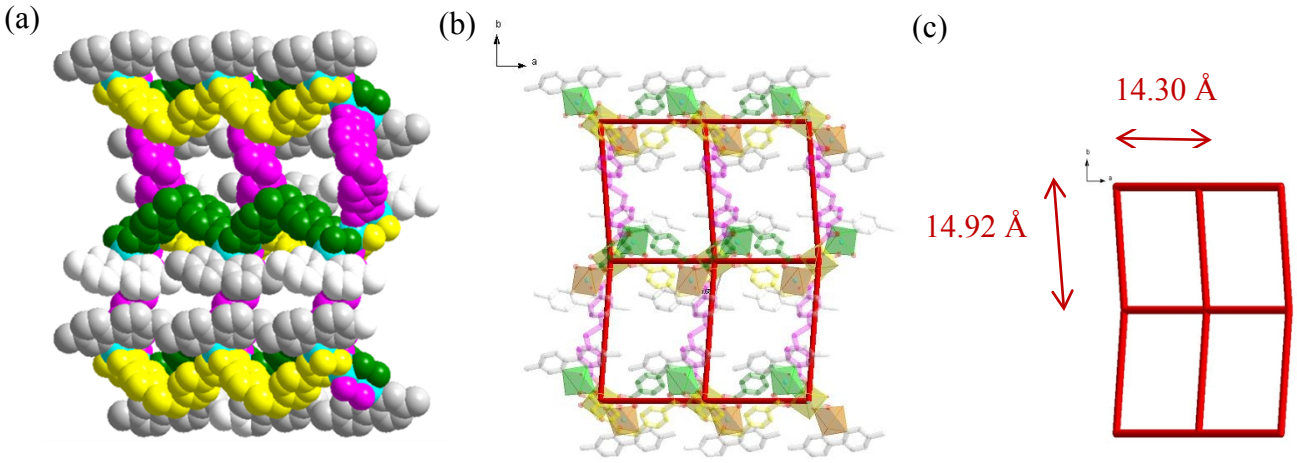

Fig. S11 The structural views of **2**: (a) showing the pore cavities in space-filling mode excluded with the van der Waals radii and the hydrogen atoms and solvent molecules are omitted for calrity; (b) schematic representation of a 2D network with a 4^4-**sql** topology; (c) showing the separation distances between the trinuclear clusters with 14.30 x 14.92 $Å^2$.

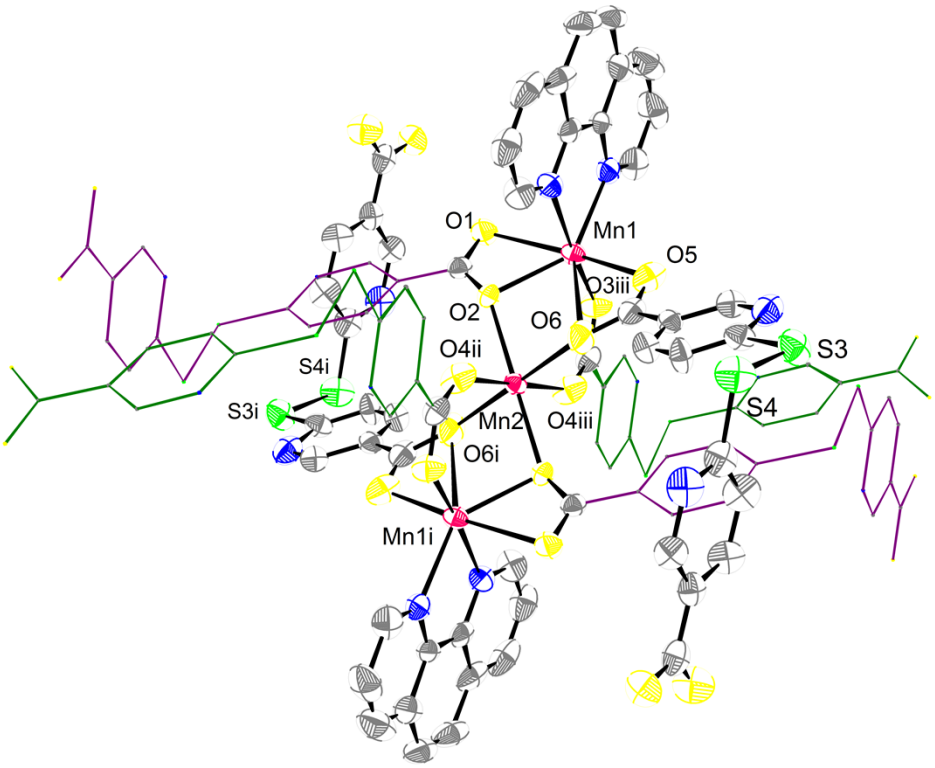

Fig. S12 The ORTEP drawing of **3** with 30% thermal ellipsoid probability. Hydrogen atoms were omitted for clarity (symmetry transformations used to generate equivalent atoms: i = 2 − x, −y, − z; ii = 1 − x, 1 − y, −z; iii = 1 + x, −1 + y, z).

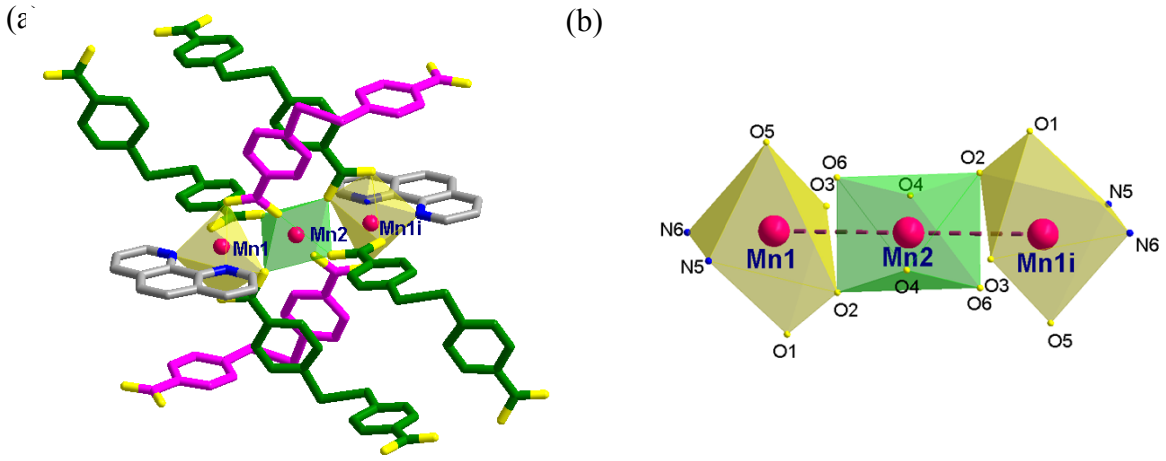

Fig. S13 Structures of **3** (symmetry transformations used to generate equivalent atoms: i = 2 −x, −y –z): (a) a schematic representation, (b) a view of trinuclear cluster in a polyhedral mode, where the Mn(II) atoms are linked by carboxylato-oxygen atoms (O2) and the separation distance of Mn1···Mn2 with 3.42 Å.

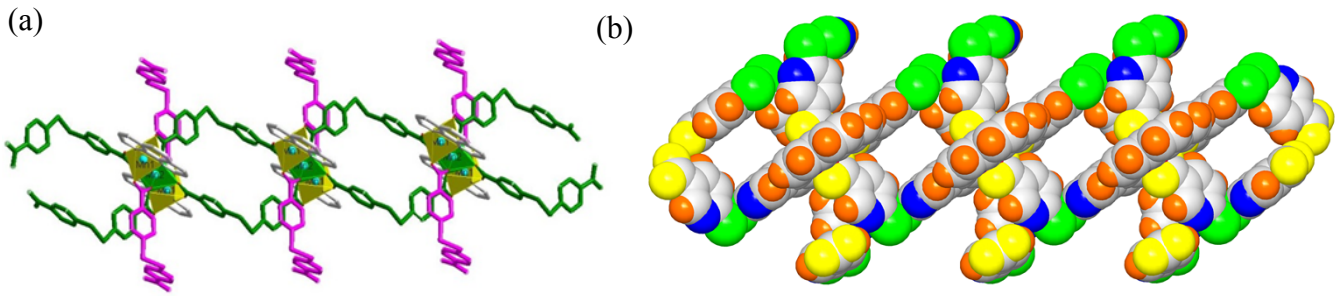

Fig. S14 A 1D double-stranded rod dangling the $Hdtdn^-$ ligands (highlighted in pink) viewed along the *c* axis (a) with a polyhedron mode, (b) with a space-filling mode (green, S; blue, N; yellow, O; grey, C; orange, H).

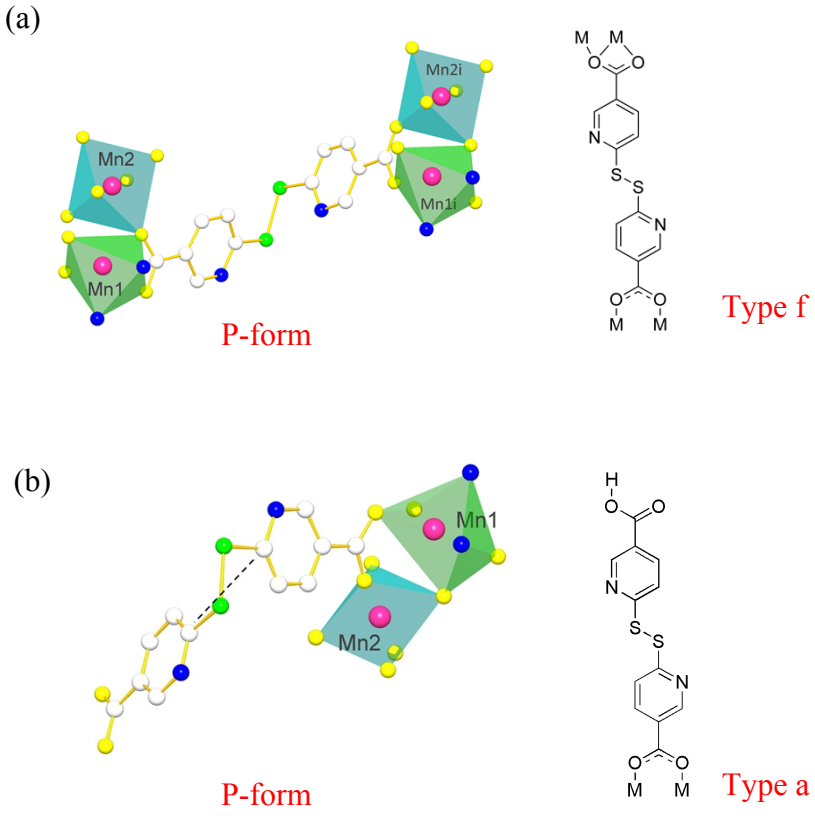

Fig. S15 The structures of **3** show the axial chirality forms, coordination modes, and torrsion angles (−C−S−S−C−) of the $dtdn^{2-}$ ligands: (a) P-form, Type (f), 104.8° and 104.7° (symmetry transformations used to generate equivalent atoms: i = −1 + x, 1 + y, z); (b) P-form, Type (a), 105.4° and 103.2°.

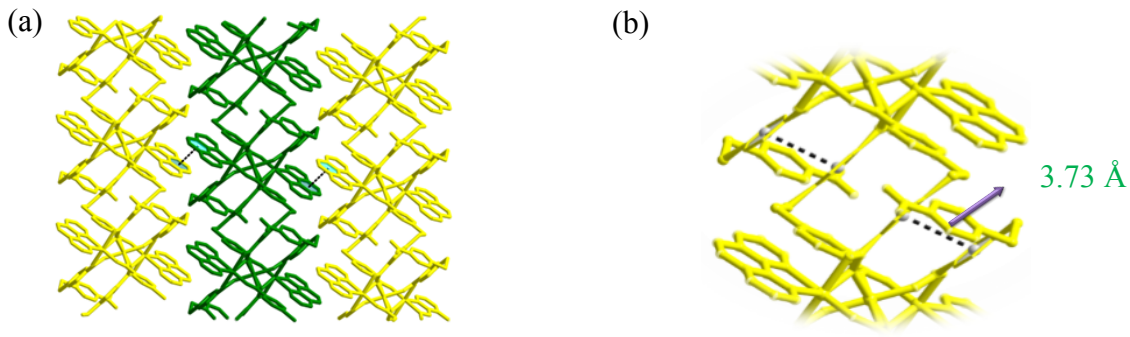

Fig. S16 The structures of **3** with the π–π stacking interactions: (a) a view of the 1D rods that are regularly stacked in an AAA manner viewed along the *a* axis; (b) connected via the adjacent pyridyl rings with 3.73(1) Å.

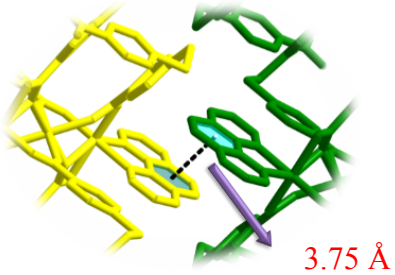

Fig. S17 The structures of **3** with the π–π stacking interactions connected via the phen rings with 3.75(1) Å.

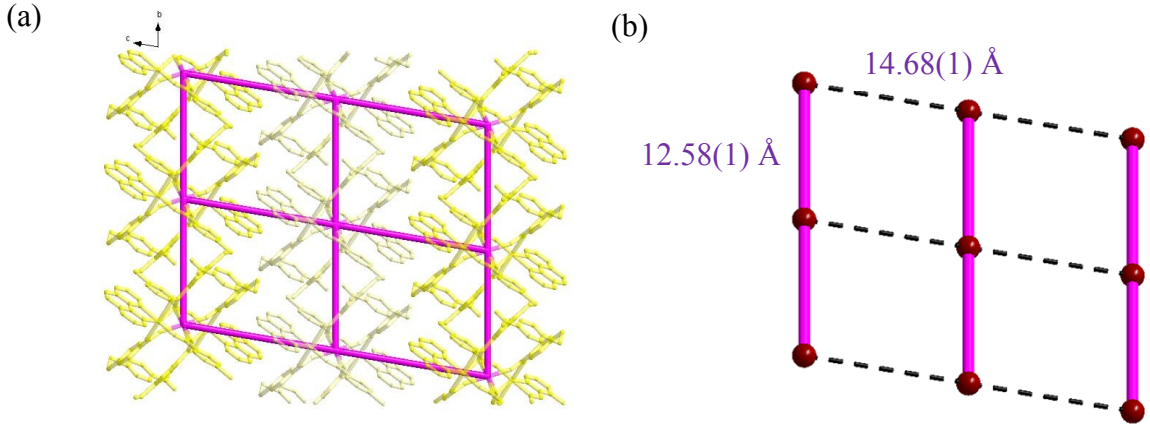

Fig. S18 (a) Showing the environments of the trinuclear cluster units of **3** with a grid-like structure. (b) A schematic view of the trinuclear custer with the separation distances of 14.68(1) x 12.58(1) $Å^2$.

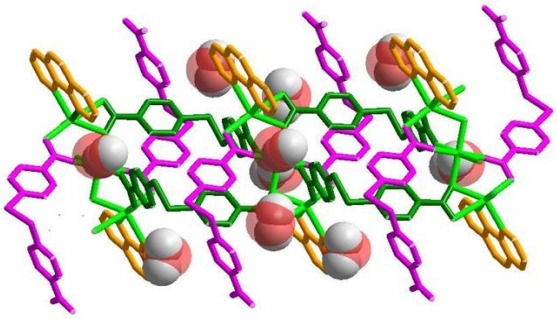

Fig. S19 Showing the guest water molecules in a space-filling mode that filled in cavities of **3**.

(a) (b)

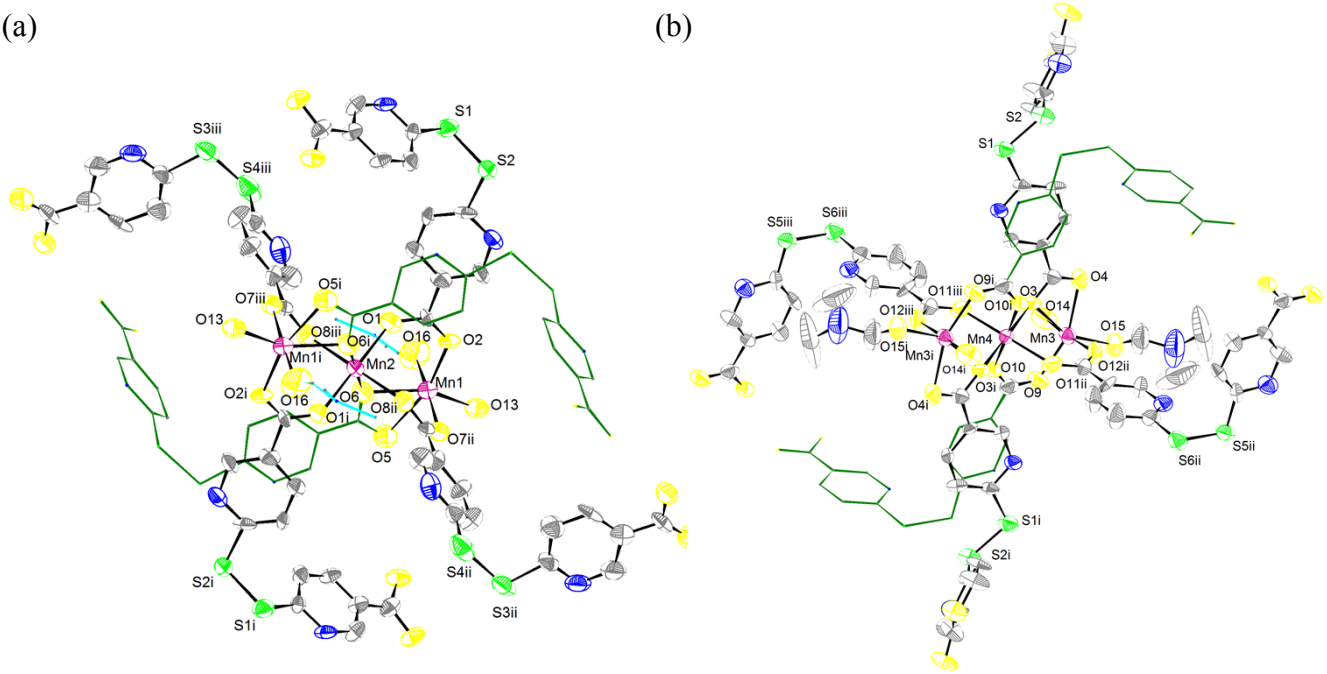

Fig. S20 Compound **4** has two kinds of trinuclear clusters with similiar environments (left and right). Hydrogen atoms were omitted for clarity (symmetry transformations used to generate equivalent atoms: for left, i = −x, 1 −y, −z, ii = −1 + x, y, z , iii = 1 −x, 1 −y, −z; for right, i = −x, −y, 1 –z, ii = −1 + x, y, z, iii = 1 −x, −y, 1−z).

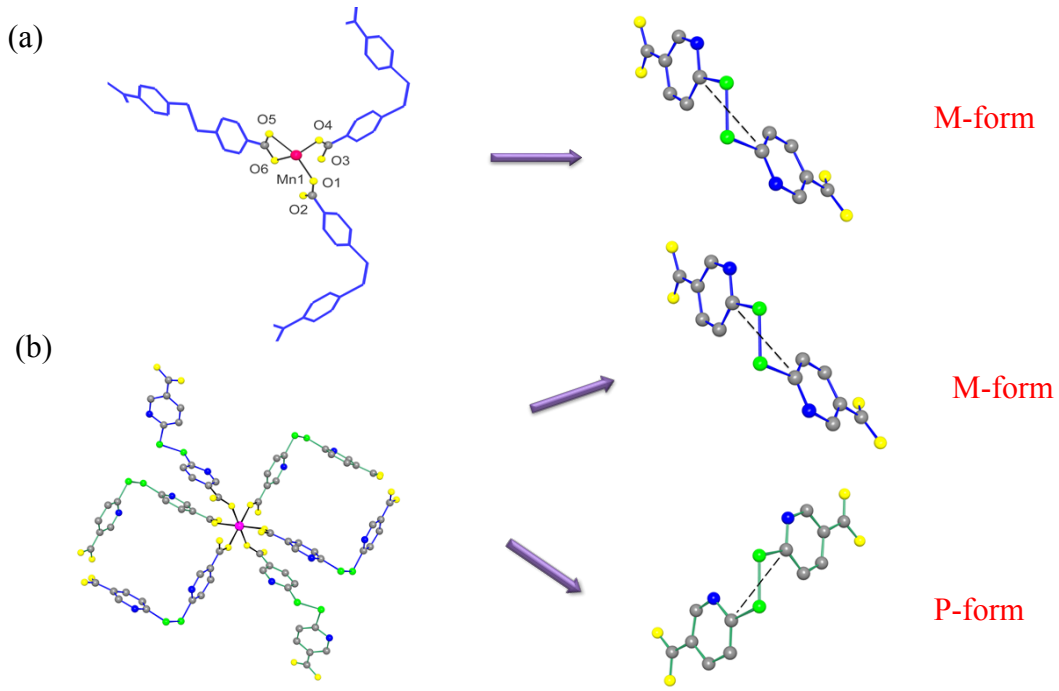

Fig. S21 Showing the chirality forms of the dtdn^{2-} ligands of **4**: (a) that are coordinated to the Mn1 atom exhibiting M-form, (b) that of the Mn2 atom display M- and P-forms.

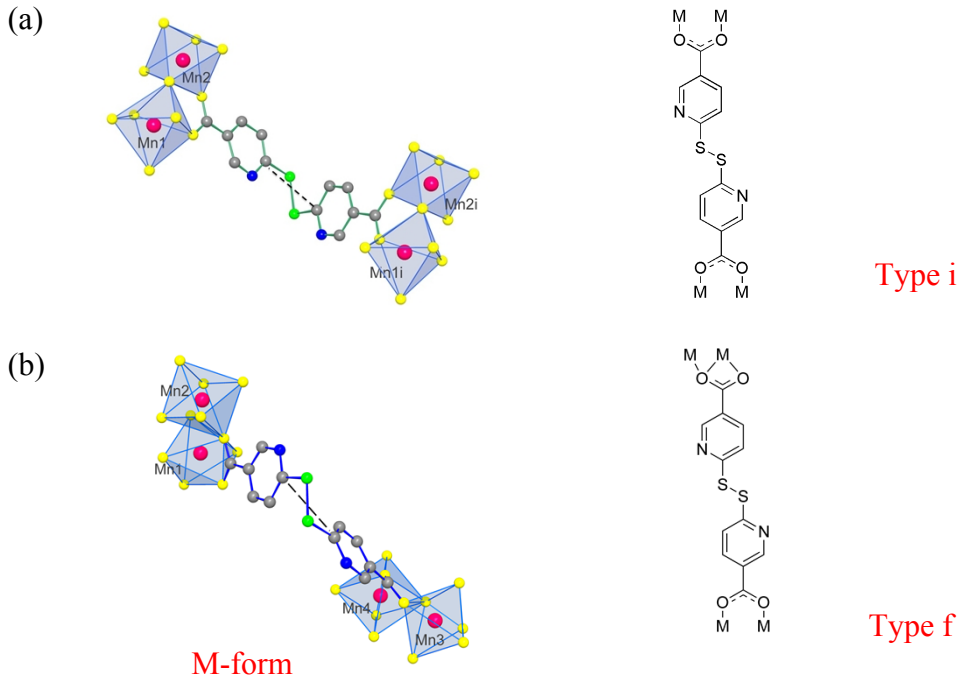

Fig. S22 The structural views of **4** show the axial chirality forms, coordination modes, and torsion angles (−C−S−S−C−) of the dtdn^{2-} ligands: (a) M-form, Type (i), 104.6° and 104.9° (symmetry transformations used to generate equivalent atoms: i = 1 + x, y, z); (b) M-form, Type (f), 103.2° and 105.8°.

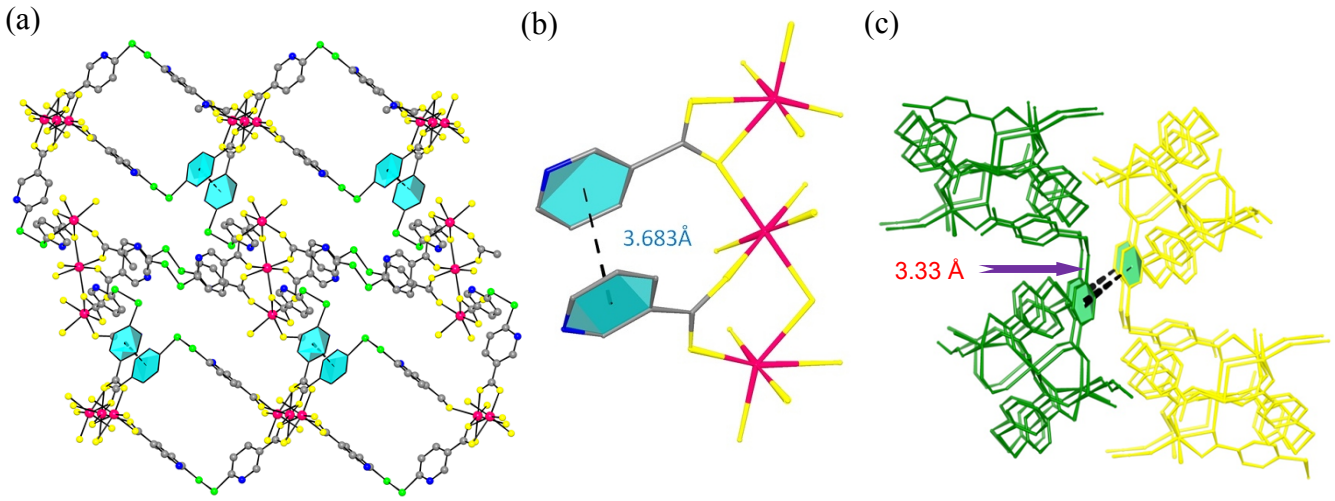

Fig. S23 (a) The adjacent layers of **4** are reguarly stacked into a 2D network. (b) Connecting through the π–π stacking interactions via intralayers with 3.68 Å. (c) Connecting via the interlayer with 3.33 Å.

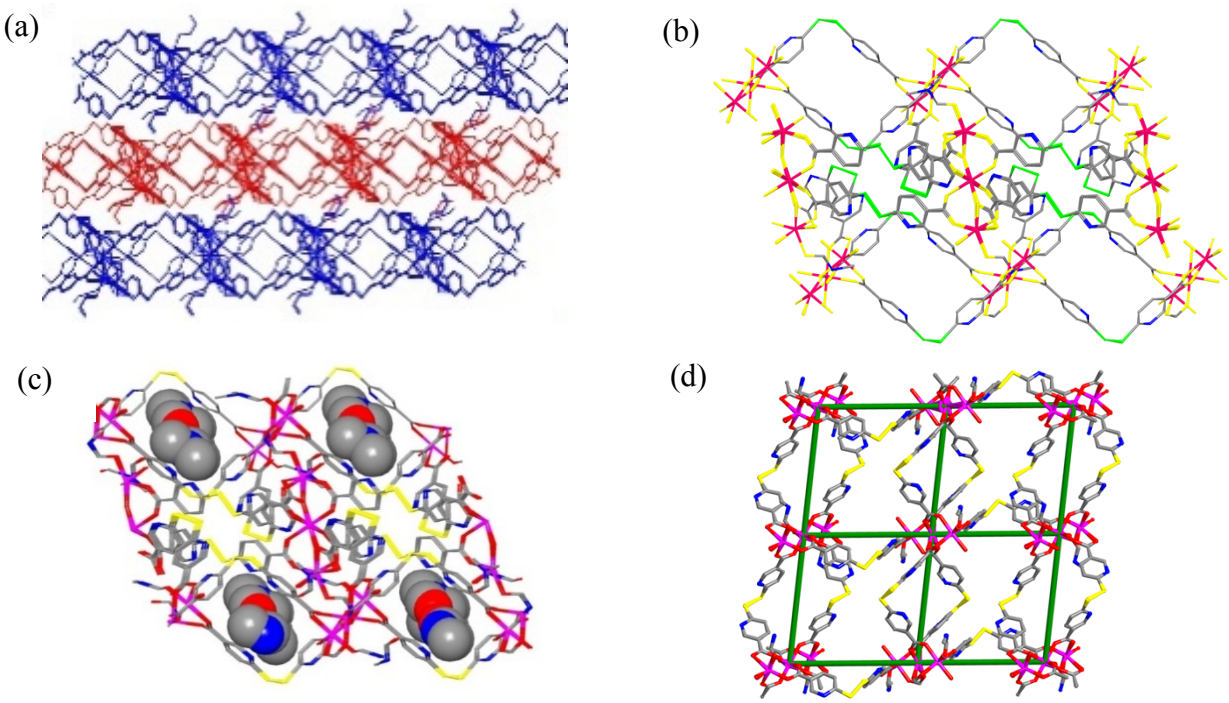

Fig. S24 (a) The 2D layers are stacked through the π–π interactions in an ABAB manner to give a 3D framework of **4** viewed along the *a* axis. (b) The 1D channels are apparent viewed along the *c* axis. (c) The guest water and DMF molecules are included in the channels. (d) The separation distances in a 2D grid network are about 12.9 x 13.5 $Å^2$.

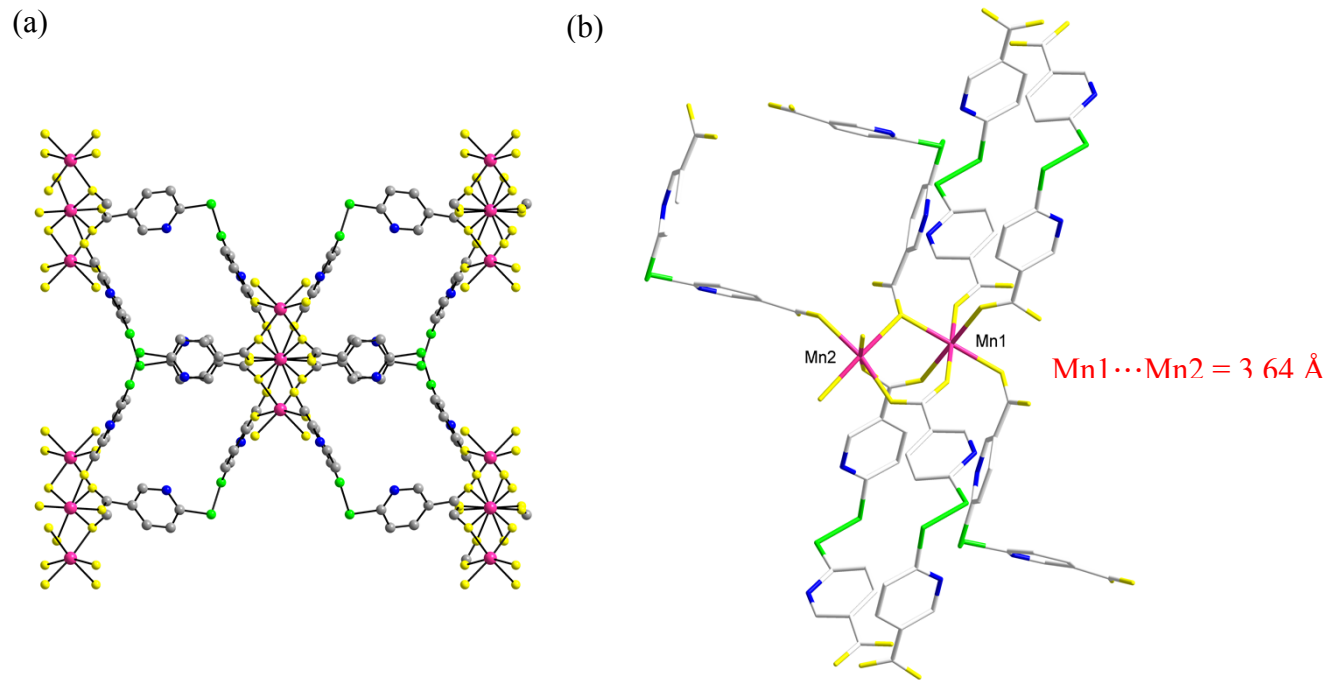

Fig. S25 (a) Coordination environments of the Mn(II) cations in the trinuclear cluster unit of **5**. Hydrogen atoms were omitted for clarity. (b) Showing an infinite zigzag metal-oxide wire that is connected via the Mn(II) ions and bridged by the carboxylates from the $dtdn^{2-}$ ligands in μ_2,η^1- and μ_2,η^2-manners viewed along the *a* axis.

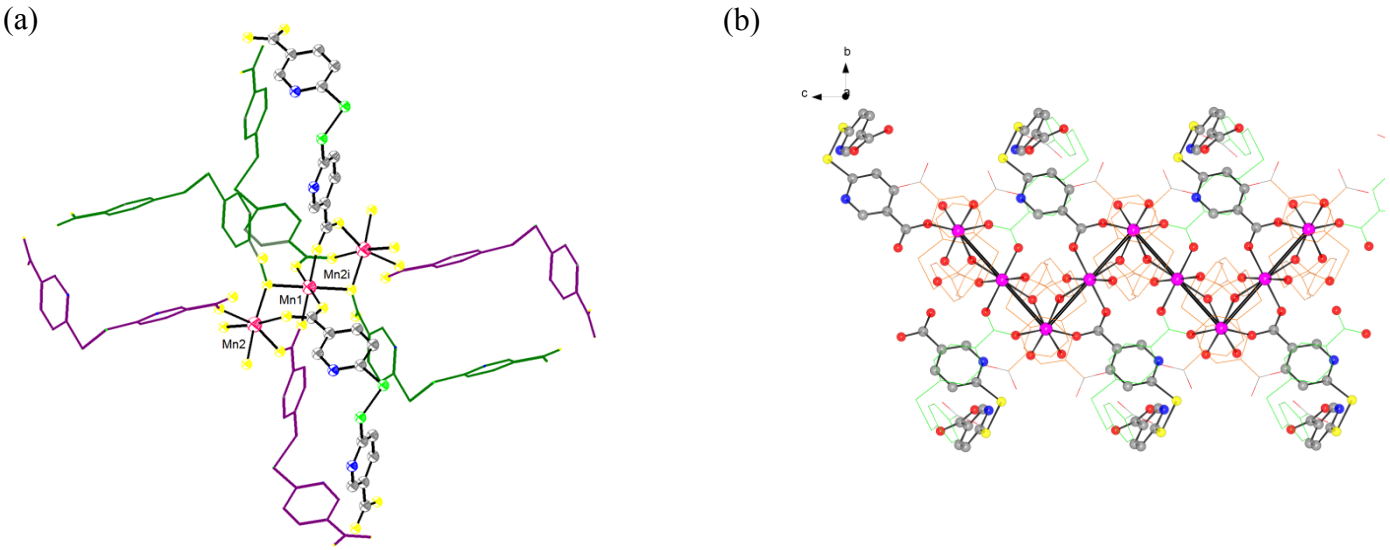

Fig. S26 (a) View of a 2D framework of **5** that is self-assembled from the manganese-oxide wires and the bridging $dtdn^{2-}$ ligands viewed along the *c* axis (symmetry transformations used to generate equivalent atoms: i = 2 −x, −y, 2 −z). (b) Showing the coordination environments of the $dtdn^{2-}$ ligands and the separation distance of Mn1···Mn2 with 3.64(1) Å in the metal-oxide wire.

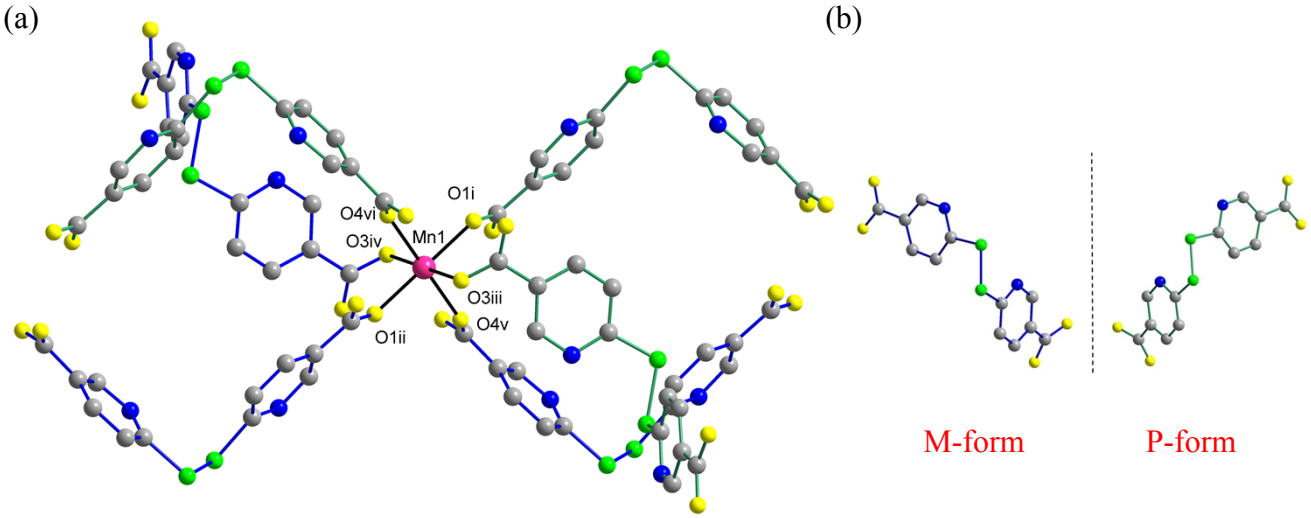

Fig. S27 Structure of compound **5**: (a) showing the coordination environments of the dtdn^{2-} ligand on the Mn1 atom (symmetry transformations used to generate equivalent atoms: i = x, y, z, ii = 2 − x, −y, 2 – z, iii = 1.5 − x, −0.5 + y, 1.5 – z, iv = 0.5 + x, 0.5 −y, 0.5 + z, v = 1.5 − x, 0.5− y, 2– z, vi = 0.5 + x, −0.5 + y, z), (b) view of the M- and P-forms.

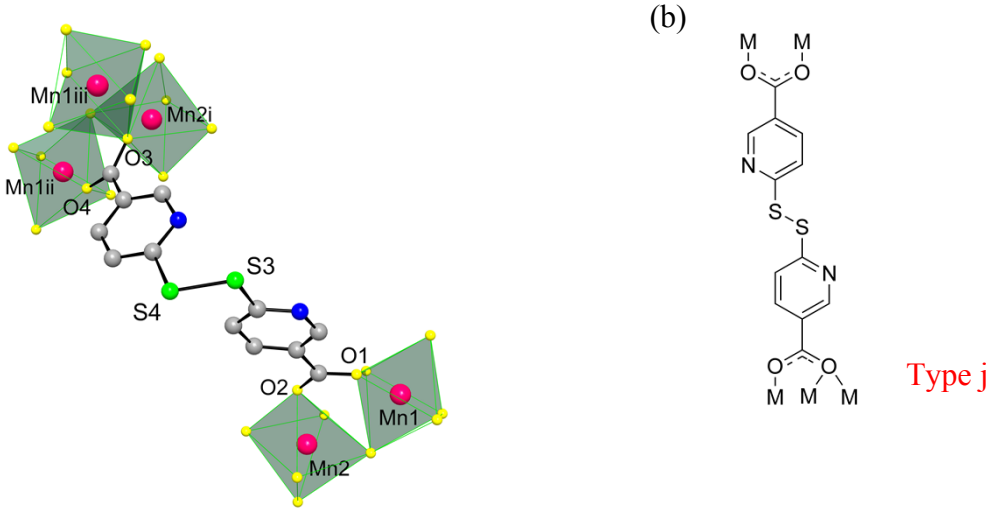

Fig. S28 (a) The dtdn^{2-} ligand is bridged between the Mn(II) cations in compound **5** (hightlighted in the polyhedron mode in pale blue color) possessses the torsion angles (C–S–S–C–) of 104.8° and 104.1° (symmetry transformations used to generate equivalent atoms: i = 1.5 −x, 0.5 −y, 2 –z; ii = −0.5 + x, 0.5 + y, z; iii = 1.5 −x, 0.5 + y, 1.5 −z), (b) view of the coordination mode of the dtdn^{2-} ligand that exhibits in Type (j).

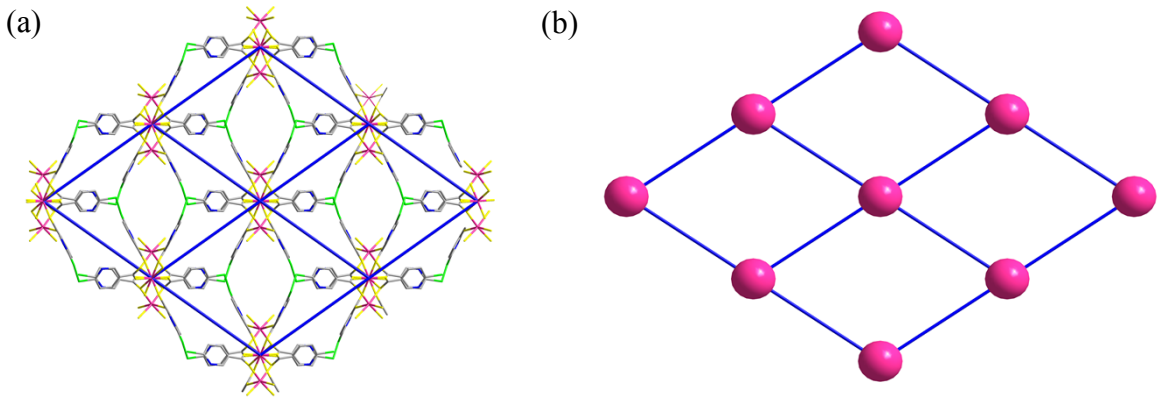

Fig. S29 The structures of **5**: (a) view of a 2D grid network, (b) the separation distance between each Mn1 center in pink of the metal-oxide wire is 13.9 Å.

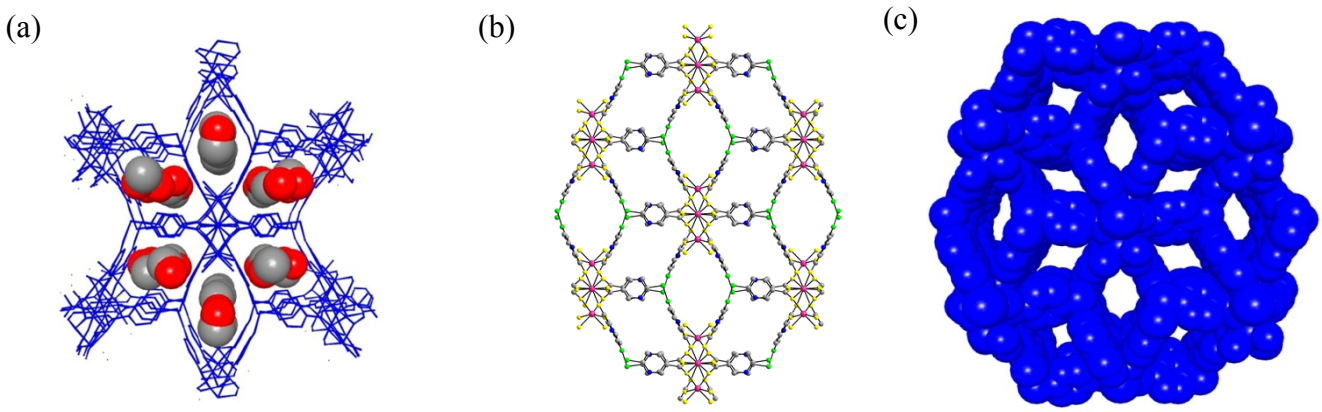

Fig. S30 Structures of compound **5**: (a) perspective 3D view along the *a* axis with embedded water molecules; (b) a 3D framework showing that the layers are packed in an AAA fashion with the π–π interactions between the pyridine motifs of the $dtdn^{2-}$ ligands; (c) a 3D packing diagram in a space-filling mode excluded with the van der Waals radii with the window sizes of 7.7 × 4.1 $Å^2$.

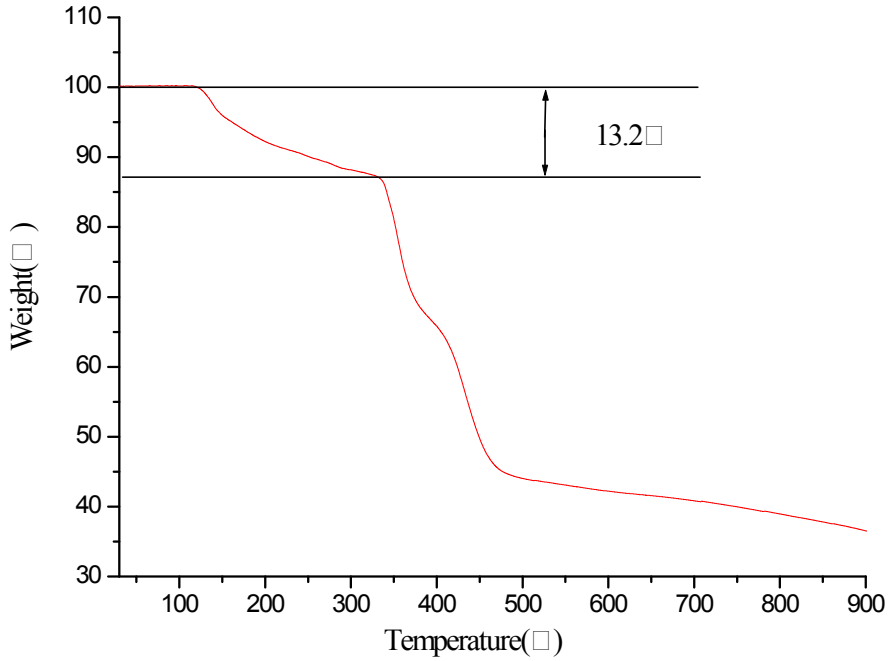

Fig. S31 Thermogravimetric analysis (TGA) curve of **1**.

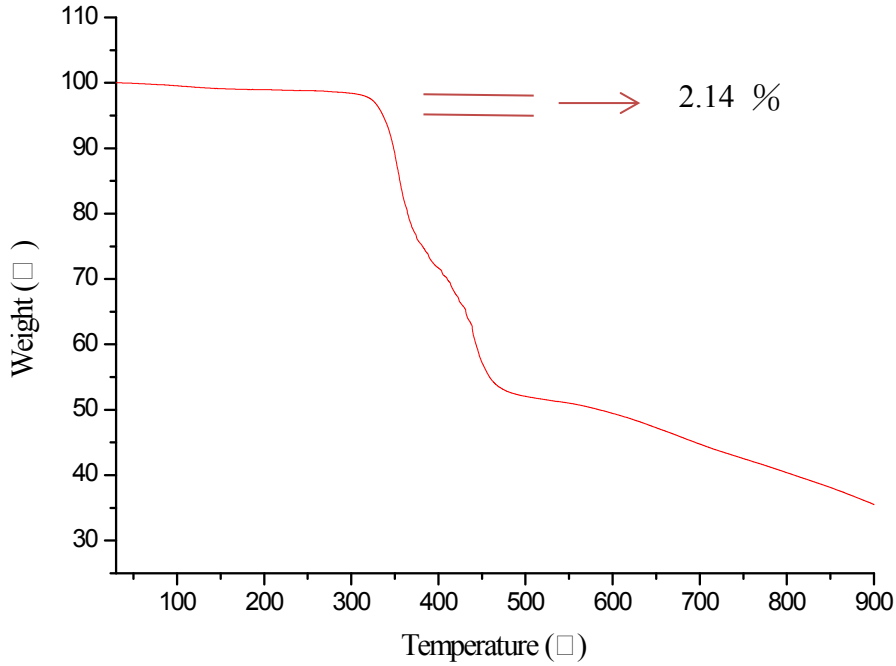

Fig. S32 Thermogravimetric analysis (TGA) curve of **2**.

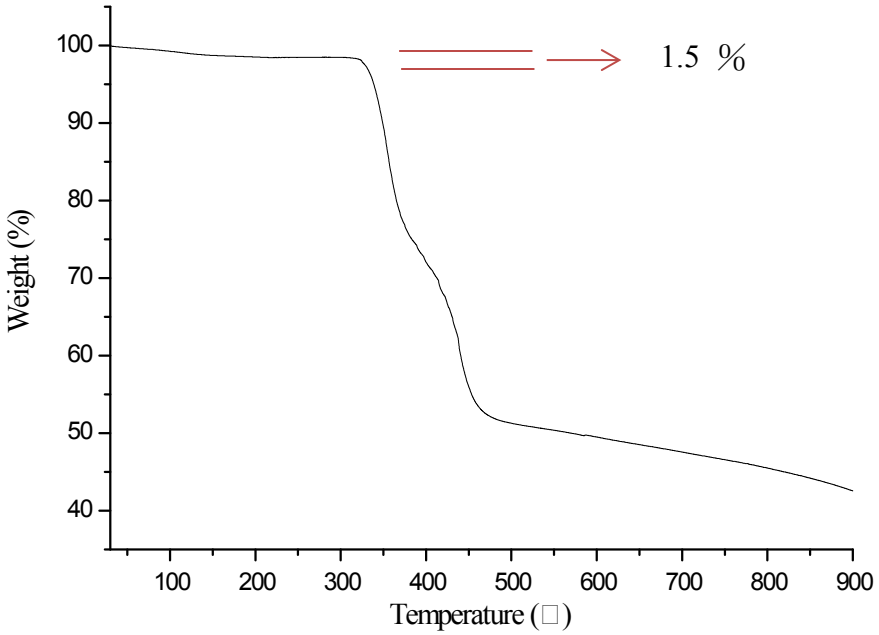

Fig. S33 Thermogravimetric analysis (TGA) curve of **3**.

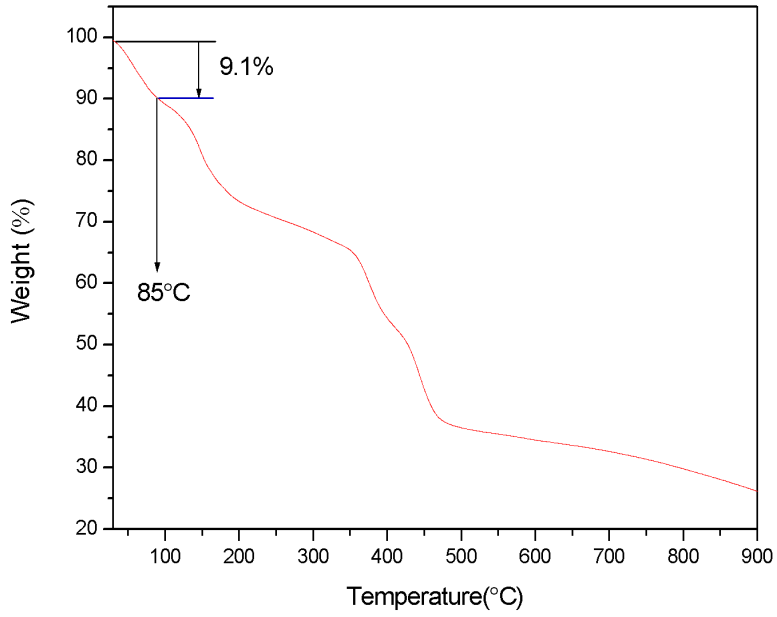

Fig. S34 Thermogravimetric analysis (TGA) curve of **4**.

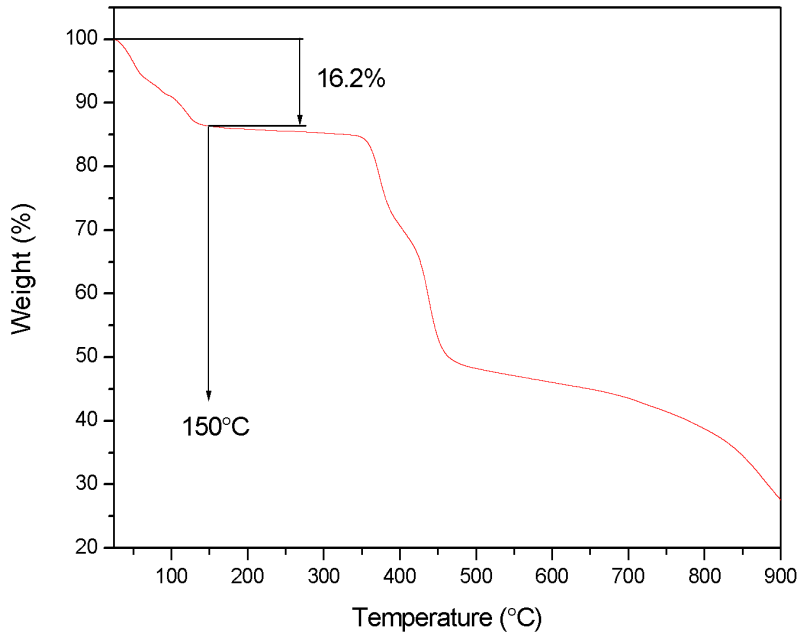

Fig. S35 Thermogravimetric analysis (TGA) curve of **5**.

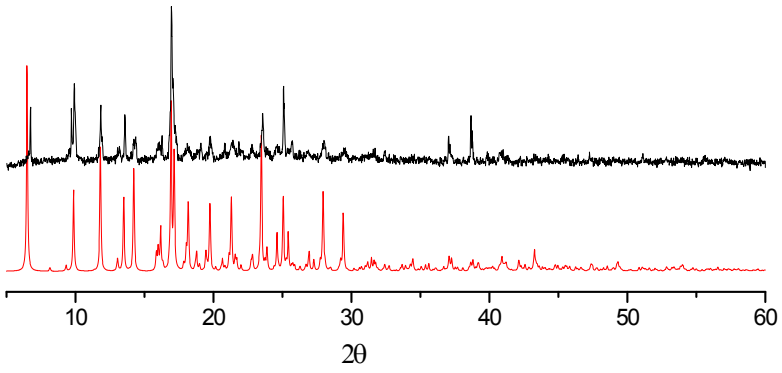

Fig. S36 Powder X-ray diffraction (PXRD) patterns for **1** (as-synthesized, black; simulated, red).

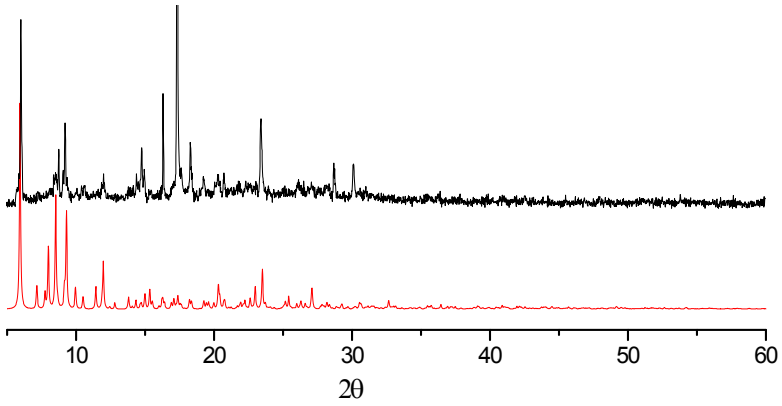

Fig. S37 Powder X-ray diffraction (PXRD) patterns for **2** (as-synthesized, black; simulated, red).

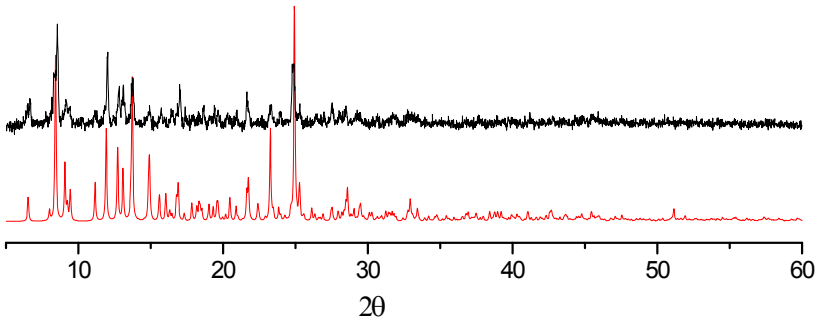

Fig. S38 Powder X-ray diffraction (PXRD) patterns for **3** (as-synthesized, black; simulated, red).

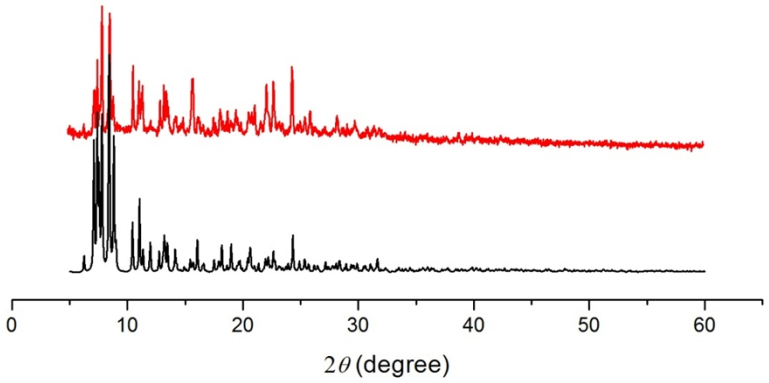

Fig. S39 Powder X-ray diffraction (PXRD) patterns for **4** (as-synthesized, black; simulated, red).

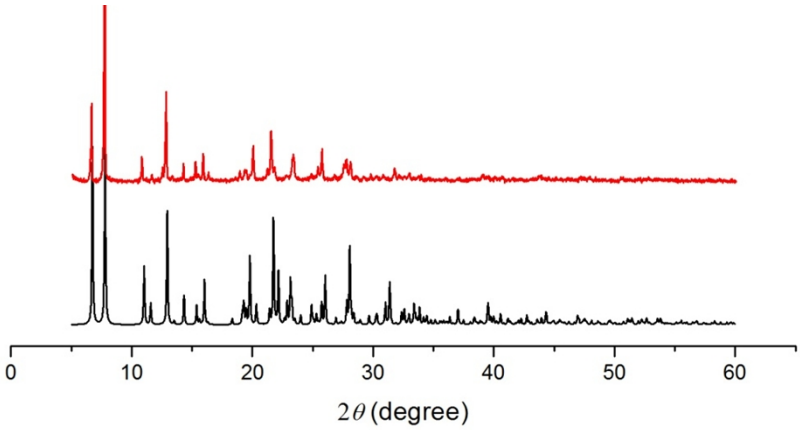

Fig. S40 Powder X-ray diffraction (PXRD) patterns for **5** (simulated, black; as-synthesized, red).

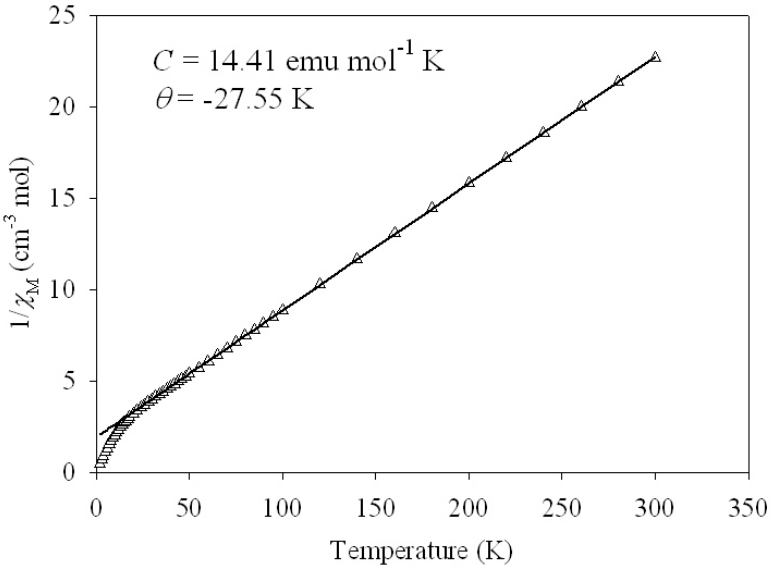

Fig. S41 Plot of $1/\chi_M$ vs. T for a powder compound **2**.

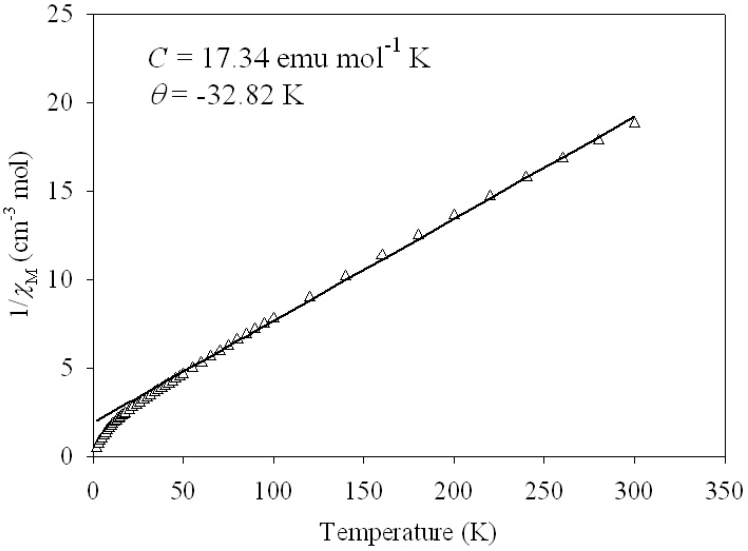

Fig. S42 Plot of $1/\chi_M$ vs. T for a powder compound **3**.

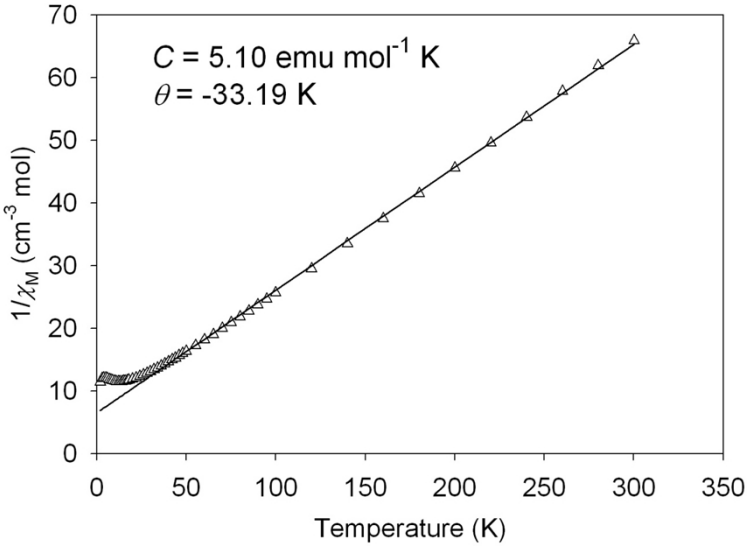

Fig. S43 Plot of $1/\chi_M T$ vs. T for a powder sample of compound **5**.

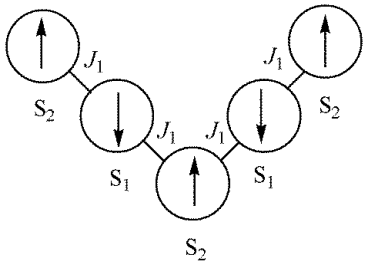

Fig. S44 Schematic presentation of spin arrangement for **5**.

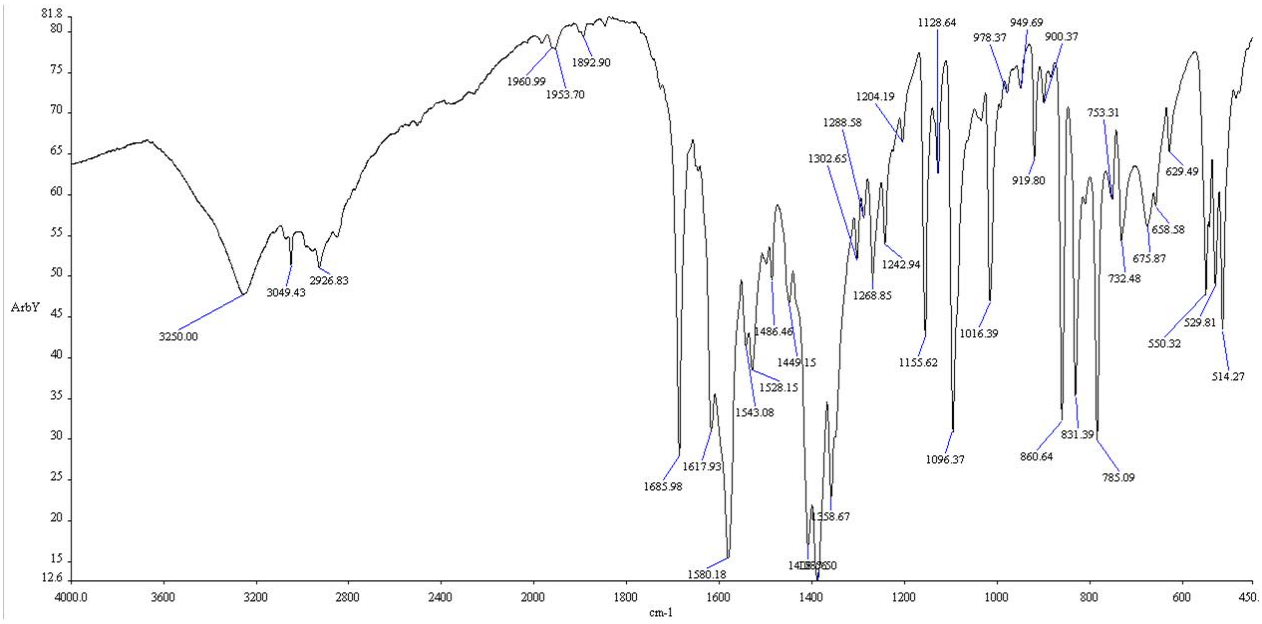

Fig. S45 IR spectrum of **1**.

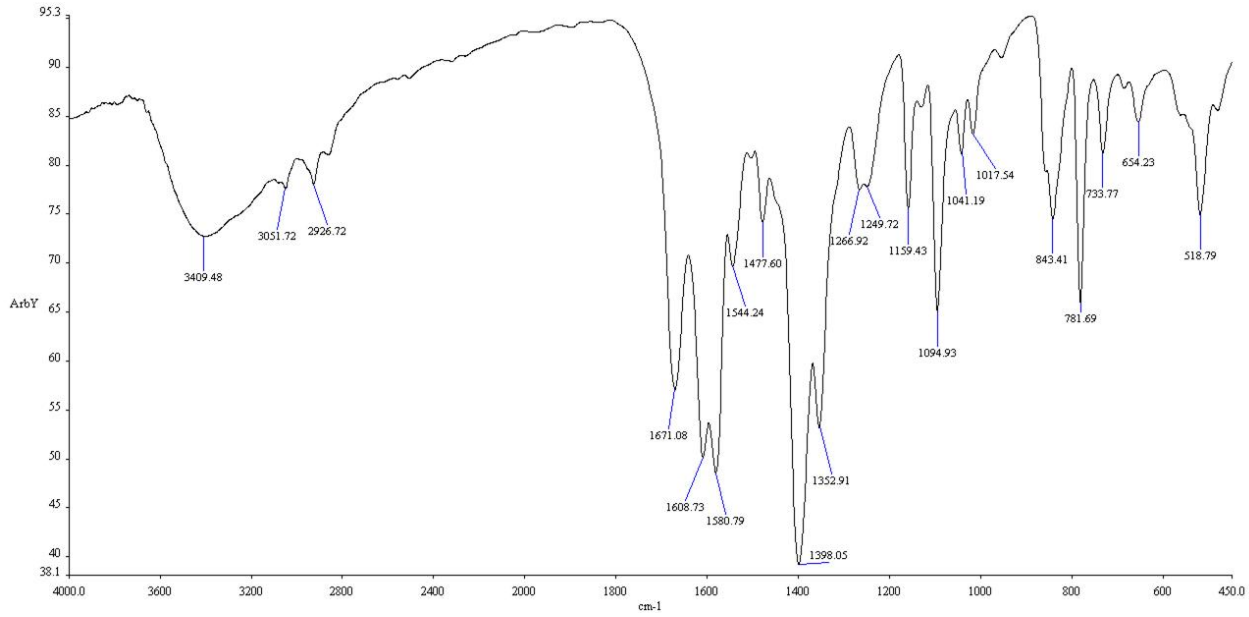

Fig. S46 IR spectrum of **2**.

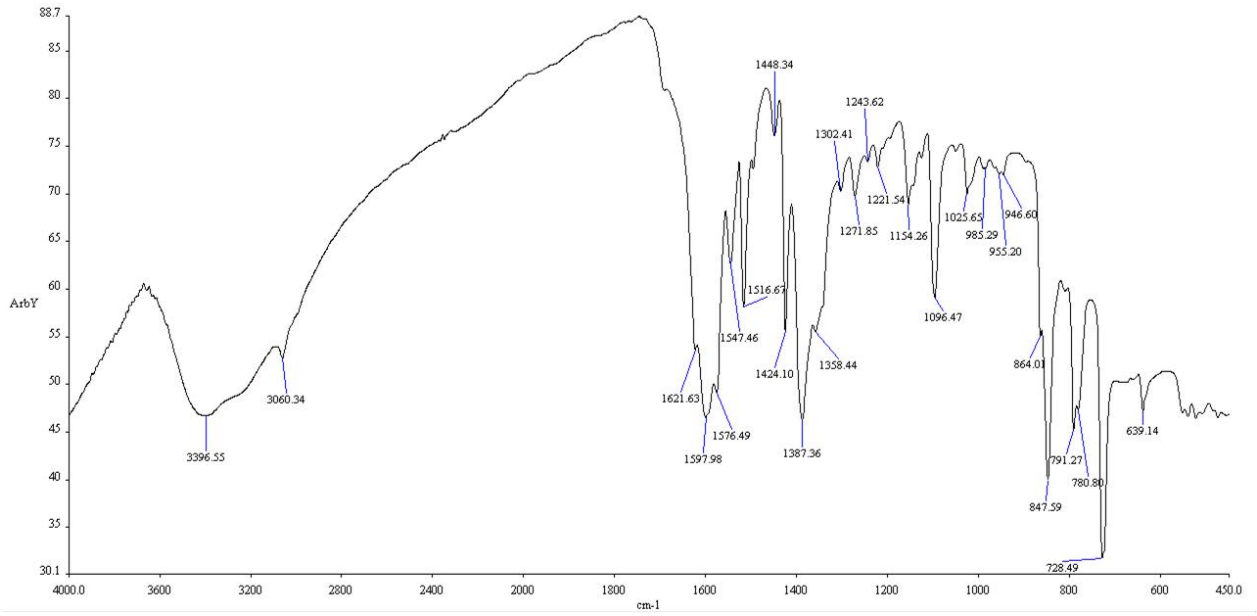

Fig. S47 IR spectrum of **3**.

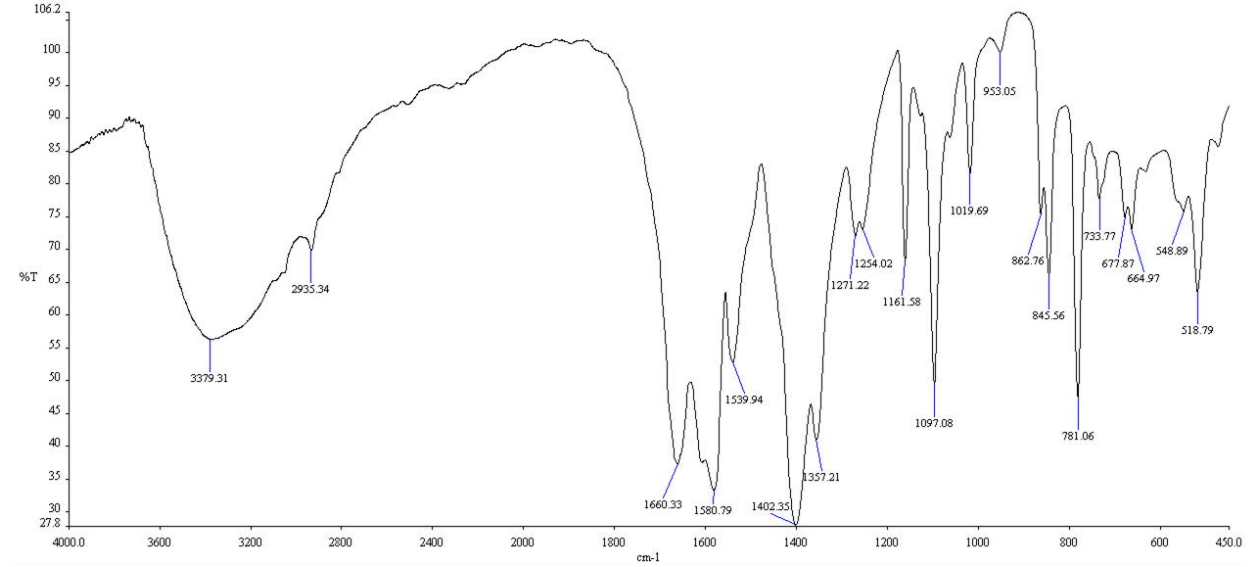

Fig. S48 IR spectrum of **4**.

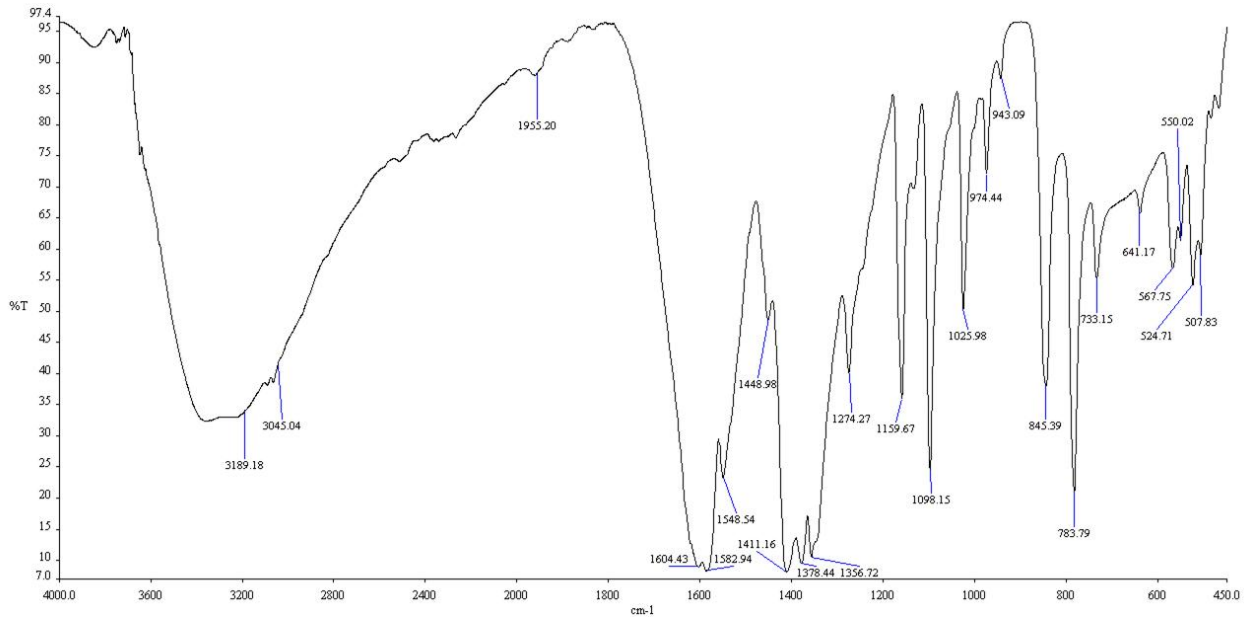

Fig. S49 IR spectrum of **5**.

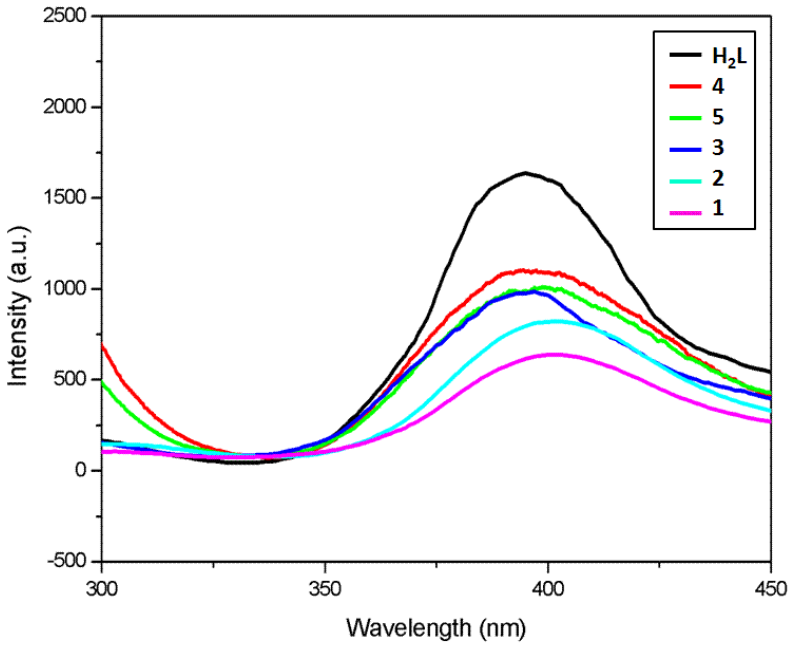

Fig. S50 Photoluminescence spectra of **1**–**5** and ligand H_2L (L = $dtdn^{2-}$) in the solid state at room temperature (excited at 240 nm).